Journal of Biomechanics 46 (2013) 1014–1020

Contents lists available at SciVerse ScienceDirect

Journal of Biomechanics

journal homepage: www.elsevier.com/locate/jbiomech
www.JBiomech.com

Bridging the gap between cadaveric and *in vivo* experiments: A biomechanical model evaluating thumb-tip endpoint forces

Sarah J. Wohlman [a,c], Wendy M. Murray [a,b,c,d,*]

[a] Department of Biomedical Engineering, Northwestern University, Evanston, IL, USA
[b] Department of Physical Medicine and Rehabilitation, Northwestern University Feinberg School of Medicine, Chicago, IL, USA
[c] Sensory Motor Performance Program, Rehabilitation Institute of Chicago, Chicago, IL, USA
[d] Edward Hines, Jr. VA Hospital, Hines, IL, USA

ARTICLE INFO

Article history:
Accepted 26 October 2012

Keywords:
Computer simulation
Thumb
Muscles
Biological models

ABSTRACT

The thumb is required for a majority of tasks of daily living. Biomechanical modeling is a valuable tool, with the potential to help us bridge the gap between our understanding of the mechanical actions of individual thumb muscles, derived from anatomical cadaveric experiments, and our understanding of how force is produced by the coordination of all of the thumb muscles, derived from studies involving human subjects. However, current biomechanical models do not replicate muscle force production at the thumb-tip. We hypothesized that accurate representations of the axes of rotation of the thumb joints were necessary to simulate the magnitude of endpoint forces produced by human subjects. We augmented a musculoskeletal model with axes of rotation derived from experimental measurements (Holzbaur et al., 2005) by defining muscle–tendon paths and maximum isometric force-generating capacity for the five intrinsic muscles. We then evaluated if this augmented model replicated a broad range of experimental data from the literature and identified which parameters most influenced model performance. The simulated endpoint forces generated by the combined action of all thumb muscles in our model yielded comparable forces in magnitude to those produced by nonimpaired subjects. A series of 8 sets of Monte Carlo simulations demonstrated that the difference in the axes of rotation of the thumb joints between studies best explains the improved performance of our model relative to previous work. In addition, we demonstrate that the endpoint forces produced by individual muscles cannot be replicated with existing experimental data describing muscle moment arms.

1. Introduction

A majority of the activities of daily living require us to use our hands to interact with the environment. Of particular importance is our ability to apply forces produced at the thumb-tip to grasp, hold, and manipulate objects as the thumb is required for 40% of hand function (Swanson, 1964).

Given the importance of force production by the thumb, biomechanical simulations have been developed to study the transformation from muscle force to thumb-tip endpoint forces in detail. However, current biomechanical models of the thumb neither replicate the thumb-tip forces produced by human subjects (Valero-Cuevas et al., 2003) nor the forces produced when individual cadaveric muscles are loaded with a known force (Pearlman et al., 2004; Towles et al., 2008). For example, Valero-Cuevas et al. (2003) developed a biomechanical model of the thumb to calculate forces produced by the coordinated actions of all thumb muscles and compared simulation results to experimental measurements of forces produced by nonimpaired subjects during maximum effort. The authors concluded that the model failed; the model was reported to be approximately four times *weaker* than human subjects. In contrast, Towles et al. (2008), implementing a biomechanical model that incorporated similar model parameters as those described by Valero-Cuevas et al., calculated the endpoint forces produced by individual muscles when they were loaded with a known force in a cadaveric experiment and reported that the simulated endpoint forces *overestimated* the forces measured in cadaveric specimens in six of nine muscles. Even with model parameters that better reflected experimental data (Hollister et al., 1992, 1995), Goehler and Murray (2010) also reported an overestimation of endpoint forces produced by some extrinsic thumb muscles. Thus, current biomechanical models of the thumb are both underestimating the forces produced by human subjects (Valero-Cuevas et al., 2003) and overestimating the force magnitude produced by individual muscles, as quantified in cadaveric specimens (Goehler and Murray, 2010; Towles et al., 2008).

* Corresponding author at: Sensory Motor Performance Program, Rehabilitation Institute of Chicago, 345 East Superior Street, Chicago, IL 60611, USA.
Tel.: +1 312 238 6965; fax: +1 312 238 2208.
E-mail address: w-murray@northwestern.edu (W.M. Murray).

0021-9290/$ - see front matter © 2012 Elsevier Ltd. All rights reserved.
http://dx.doi.org/10.1016/j.jbiomech.2012.10.044

As reported in the literature, it is not clear which biomechanical parameters (i.e. description of joint axes of rotation, muscle moment arms, or maximal isometric forces) most influence the transformation from muscle force to thumb-tip endpoint force. Because their study thoroughly evaluated the sensitivity of their simulations to variability in other musculoskeletal parameters (muscle moment arms or maximal isometric forces), Valero-Cuevas et al. (2003) speculated that the discrepancy between model results and experimental data measured from human subjects during maximum effort was primarily due to the simplified representation of the axes of rotation of the thumb joints implemented in their model. In contrast, both Towles et al. (2008) and Goehler and Murray (2010) discussed how altering muscle moment arms resulted in improved simulation of thumb-tip endpoint forces for individual muscles. Importantly, none of these studies evaluated model performance relative to both the thumb-tip forces produced by human subjects (where a net force produced by coordinated muscle action is measured) and the forces produced when individual cadaveric muscles are loaded with a known force.

The objectives of this study are: (1) to develop a biomechanical model of the thumb to investigate the transformation between muscle force and thumb-tip endpoint force for both individual muscles and the net force produced via combined muscle actions and (2) to evaluate which subset of biomechanical parameters has the most influence on model simulations. In this study, we augmented the model previously described by Holzbaur et al. (2005) to include the muscle–tendon paths and the maximum isometric force-generating capacity of the five intrinsic muscles, where the geometry of each muscle–tendon path was optimized to replicate the mechanical action of a given intrinsic muscle (Pearlman et al., 2004). We then evaluated how accurately this augmented model replicated a broad range of experimental data and performed a series of 8 sets of Monte Carlo simulations to evaluate the relative influence of different biomechanical parameters. Based on what was first speculated by Valero-Cuevas et al. (2003), we hypothesized that simulations would be most sensitive to the description of the axes of rotation, as compared to either muscle moment arms or maximum isometric forces.

2. Methods

We augmented a musculoskeletal model of the thumb (Holzbaur et al., 2005) by defining the muscle–tendon paths and the maximum isometric force-generating capacity of the five intrinsic muscles including abductor pollicis brevis (APB), the transverse and oblique heads of adductor pollicis (ADPt and ADPo, respectively), flexor pollicis brevis (FPB), and opponens pollicis (OPP). The musculoskeletal model described by Holzbaur et al. (2005) defined four degrees of freedom at the thumb, which were derived from experimental measurements of the kinematics (Hollister et al., 1992, 1995). The model includes two degrees of freedom at the carpometacarpal (CMC) joint (flexion/extension and abduction/adduction), one degree of freedom at the metacarpophalangeal (MCP) joint (flexion/extension), and one degree of freedom at the interphalangeal (IP) joint (flexion/extension). The previously published model defined the muscle–tendon paths of the four extrinsic thumb muscles: abductor pollicis longus (APL), extensor pollicis brevis (EPB), extensor pollicis longus (EPL), and flexor pollicis longus (FPL). The muscle–tendon paths in this model were developed to replicate the moment arms of the extrinsic muscles that have been quantified experimentally (Smutz et al., 1998).

Table 1
Joint postures for lateral and opposition pinch based on general coordinates of previously described model of upper extremity (Holzbaur et al., 2005).

Joint	Pinch
	Lateral
CMC flexion	20°
CMC abduction	−25°
MCP flexion	−45°
IP flexion	−10°
	
	Opposition
CMC flexion	20°
CMC abduction	20°
MCP flexion	−10°
IP flexion	−45°
	

*Positive angles indicate extension or abduction.

2.1. Definition of muscle–tendon paths for the intrinsic muscles

To define muscle–tendon paths for the intrinsic thumb muscles, we implemented an optimization algorithm (Yeo et al., 2011) that varied the location of the origin and insertion points for a given muscle until the final modeled path minimized the difference between the thumb-tip endpoint force calculated using our biomechanical model and experimental data describing the thumb-tip forces produced by that muscle in cadaveric testing (Pearlman et al., 2004).

The errors between simulated and experimental thumb-tip endpoint forces for lateral and opposition pinch postures (Table 1) were minimized simultaneously using a non-linear least squares optimization routine (Matlab, lsqnonlin) with the following cost function:

$$\min_{d} \sum_{i=1}^{2} \|\mathrm{F}_i - \hat{F}_i(d)\|^2 \tag{1}$$

where d is the 6×1 vector of 3D origin and insertion points, F_i the 6×1 vector of experimental thumb-tip endpoint forces, and $\mathrm{F}_i(d)$ the 6×1 vector of simulated thumb-tip endpoint force (Yeo et al., 2011).

For each iteration of the optimization algorithm for a given muscle (Fig. 1), we calculated the endpoint forces produced at the thumb-tip by that muscle in both lateral and opposition pinch posture. To calculate the force produced at the thumb-tip, we used the principle of virtual work to relate the joint torques produced by the muscle of interest for a specified level of muscle force to the resulting force at a point of interest on the distal phalanx:

$$\overline{F}_{\text{individual}} = \left[J^T\right]^{-1} \overline{L}_{\text{MA}} f_{\text{muscle}} \tag{2}$$

where $F_{\text{individual}}$ is the 3×1 endpoint force vector; J the 3×3 Jacobian matrix; L_{MA} the 3×1 muscle moment arm vector; and f_{muscle} is the given force of the muscle of interest (Goehler and Murray, 2010). Because none of the intrinsic muscles cross the IP joint, it was only necessary to transform joint torques produced about the three remaining degrees of freedom, creating a square Jacobian matrix. The torques produced by a muscle about the CMC and MCP joints were calculated as the product of the muscle's moment arms about those joints and the specified level of muscle force. Because muscle moment arms vary with the geometry of the muscle–tendon path, L_{MA} was re-calculated in each iteration of the optimization. The origin and insertion coordinates were transformed to muscle moment arm via the partial velocity method (Delp and Loan, 1995). We constrained the optimized points to be anatomically relevant (i.e. not bisect bone) in lateral and opposition pinch postures. In some cases, additional muscle points were needed to connect the optimized muscle points to the bone. These additional points were implemented so that they did not influence the moment arm calculation. For all iterations of the algorithm, muscle force was specified to replicate the load applied to that muscle in experimental cadaveric study (Pearlman et al., 2004).

2.2. Combined muscle simulations

To simulate the forces produced by nonimpaired subjects during maximal effort we replicated the methodology of Valero-Cuevas et al. (2003). Specifically, we (i) utilized linear programming to find the activation level of each muscle, so that the combined actions of all thumb muscles generated the maximum force in a specific direction and (ii) performed Monte Carlo simulations so our simulation results incorporated the variability of model parameters observed in the literature (moment arms and maximal muscle forces) and uncertainty in joint angle measurements (Valero-Cuevas et al., 2003). Our simulations included the five intrinsic muscles, as described in the previous section, and the four extrinsic muscles, defined by Holzbaur et al., with endpoint forces as described by Goehler and Murray.

We used linear programming (Matlab, linprog) to solve for muscle activation patterns that specified the contribution of each muscle to the total thumb-tip endpoint force and torque produced in five distinct directions (Fig. 2). The thumb-tip endpoint force produced by the coordinated action of all thumb muscles is:

$$\overline{F}_{\text{combined}} = [\mathrm{C}]\overline{a} \tag{3}$$

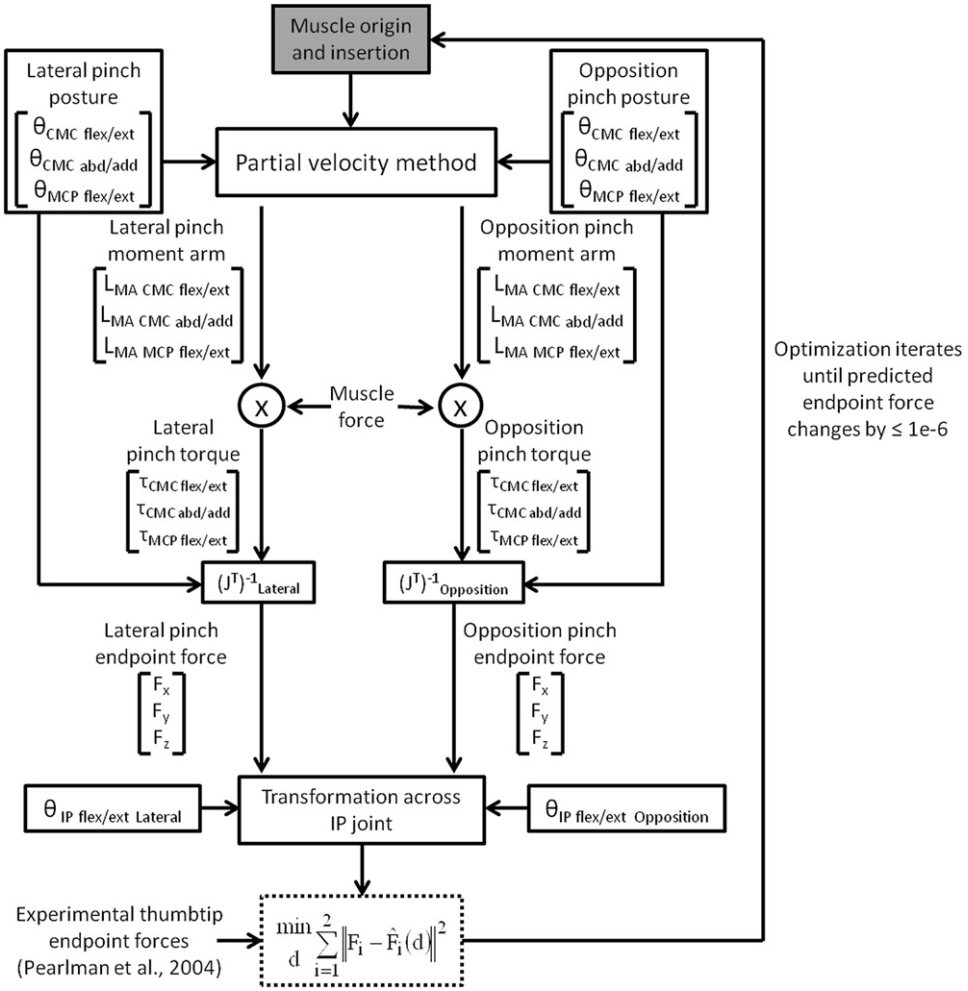

Fig. 1. Flowchart of muscle path optimization routine. The optimization begins with an initial guess for origin and insertion (gray box). Using the partial velocity method and joint postures, moment arms were calculated for lateral and opposition pinch. Moment arms were multiplied with muscle force to calculate lateral and opposition pinch torque, which was transformed into endpoint force through the inverse transpose of the Jacobian. The difference between calculated and experimental thumb-tip endpoint force is minimized (dashed box) by adjusting muscle origin and insertion. The optimization continues until it reaches convergence: the predicted endpoint force changes by less than or equal to 1e-6.

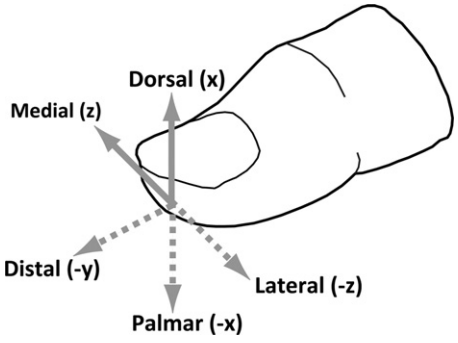

Fig. 2. Force directions at the thumb-tip.

where

$$[C] = \left[J^T\right]^{-1}[\overline{L}_{MA}][f_{max}] = \begin{bmatrix} F_{x1} & \dots & F_{x9} \\ F_{y1} & \dots & F_{y9} \\ F_{z1} & \dots & F_{z9} \\ \tau_{z1} & \dots & \tau_{z9} \end{bmatrix} \quad (4)$$

[C] is the matrix product of:

(i). the inverse transpose of the 4×4 Jacobian matrix ($(J^T)^{-1}$) relating torques produced about the four degrees of freedom to the endpoint forces and the torque about the z-axis produced at the distal phalanx,

(ii). the 4×9 matrix (L_{MA}) describing the posture-dependent moment arms of each of the 9 muscles for the four degrees of freedom, and

(iii). the 9×9 diagonal matrix (f_{max}) specifying the maximum isometric force generating capacity for each muscle.

Because the Jacobian matrix is dependent on the kinematic description of the thumb and there are four degrees of freedom, we solved for 3 components of the endpoint force and the endpoint torque about the z-axis to utilize a square matrix. In this implementation, L_{MA} also includes a representation of the extensor hood, which creates a moment arm about the IP joint for APB and ADPo during force-generation of the EPL (Valero-Cuevas et al., 2003). Maximum isometric forces for the extrinsic muscles were scaled from the values estimated from cadaveric studies reported in Holzbaur et al. (2005) using newer data that describes muscle volumes measured via MRI (Holzbaur et al., 2007a) and joint moments produced during maximum effort (Holzbaur et al., 2007b) in the same healthy subjects. Because these more recent studies did not include the intrinsic muscles, we applied the specific tension derived from those studies (50.8 N/cm^2; Mogk et al., 2011) to the muscle physiological cross sectional area (PCSA) measured in cadaveric specimens (Jacobson et al., 1992) to define maximum isometric force for the intrinsic muscles.

For a given direction (e.g. dorsal, or the $+$x direction), we solved for the activations that simulated the magnitude of the maximum force produced at the thumb-tip. In canonical form, the linear programming problem for the palmar direction is:

$$\text{Maximize}: \begin{bmatrix} F_{x1} & \dots & F_{x9} \end{bmatrix}\overline{a}$$

$$\text{Subject to}: \begin{bmatrix} F_{y1} & \dots & F_{y9} \\ F_{z1} & \dots & F_{z9} \\ \tau_{z1} & \dots & \tau_{z9} \end{bmatrix}\overline{a} \le B$$

and $0 \le a_i \le 1$ for all i, where the 1×9 vector and 3×9 matrix illustrated above correspond to the appropriate rows of matrix [C] for the direction of interest, a is 1×9 vector defining muscle activations, and B is a 3×1 vector where the first two components constrain the force produced in the directions perpendicular to the desired direction to be less than 17% of the maximum magnitude of the desired direction and the third component constrains the maximum torque about the z-axis to be less than or equal to 0.05 Nm (Valero-Cuevas et al., 2003).

The sensitivity of the maximum forces produced at the thumb-tip to variability in moment arms and maximal muscles forces, and uncertainty associated with joint angle measurement was evaluated via Monte Carlo simulation (5000 iterations). To ensure the force magnitude in each direction converged to a solution, we verified that the mean of the last 10% of iterations were within 2% of the final mean. Separate simulations were run for lateral and opposition pinch. The linear programming problem described above was solved in each iteration to find muscle activations that produced the maximal possible forces for a given sample of model parameters and joint angles. All model parameter values were varied in each iteration, using a normal distribution. The range of variability explored in the Monte Carlo simulations was based on standard deviations reported in experimental studies: muscle moment arms (Smutz et al., 1998), joint angles (Valero-Cuevas et al., 2003), and PCSAs (Jacobson et al., 1992). We constrained joint angles to be within their physiological ranges of motion and PCSA to always be non-zero.

2.3. Sensitivity of force magnitudes to different parameter sub-spaces

The sensitivity of the maximum forces produced at the thumb-tip was evaluated by repeating the Monte Carlo simulations described above under a variety of conditions. Specifically, we examined sensitivity to three different parameter sub-spaces: description of the thumb joints' axes of rotation, muscle moment arms, and muscle maximal forces (Table 2). We completed 2^3 sets of Monte Carlo simulations to evaluate every possible combination of the parameters of interest. In four sets of the Monte Carlo simulations, the joints' axes of rotation incorporated in the model were those described by Holzbaur et al. In the remaining four, we implemented a more simplified version of the joints' axes of rotation, comparable to that described by Valero-Cuevas et al., including 5 hinge joints with axes of rotation directed orthogonally to the appropriate anatomical planes and with intersecting axes of rotation for the flexion/extension and abduction/adduction degrees of freedom at the CMC and MCP joints. For each of the kinematic models, we repeated simulations using either the combination of extrinsic and intrinsic muscle moment arms implemented throughout our study or moment arms values extracted from the literature (Smutz et al., 1998). We varied the values for maximum isometric muscle force from those defined above to estimates derived from measurements of PCSA from cadaveric specimens (Jacobson et al., 1992) using a specific tension of 35.4 N/cm^2 (Brand et al., 1981). Each of the 8 sets of Monte Carlo simulations included 5000 iterations, in which all moment arm and maximum isometric muscle force parameters were varied simultaneously, using a normal distribution based on experimental variability.

Table 2
Different parameter sub-spaces.

Joint axis of rotation	Moment arms	Maximal muscle forces
Experimentally based[a]	Literature[b]	Imaging[c]
Orthogonal to anatomical planes with intersecting axes of rotation for flexion/extension and ab/adduction of CMC and MCP joints	Model (extrinsic modeled from Smutz et al.; intrinsic from muscle path optimization)	Cadaveric[d]

[a] Hollister et al. (1992, 1995).
[b] Smutz et al. (1998).
[c] Holzbaur et al. (2007a, 2007b).
[d] Jacobson et al. (1992).

3. Results

Using joint kinematics based on experimentally measured axes of rotation, maximum isometric muscle forces derived from MRI and strength data from human subjects, and the muscle moment arms described in Section 2, the simulated thumb-tip endpoint forces generated by the combined action of all thumb muscles yielded comparable forces in magnitude to those produced by nonimpaired subjects (Valero-Cuevas et al., 2003). In these simulations, the mean force magnitudes calculated from 5000 Monte Carlo simulations were on average 1.2 times stronger than human subject data in lateral pinch and equivalent in strength in opposition pinch (Fig. 3). The mean force magnitude produced at the thumb-tip fell within one standard deviation of the experimental data in three of five force directions for both lateral pinch posture and opposition pinch posture.

The muscle–tendon paths for the intrinsic thumb muscles that resulted from the optimization process yielded muscle moment arms that differed substantially from muscle moment arms measured in cadaveric specimens (Smutz et al., 1998) in both the lateral pinch and opposition pinch postures (Fig. 4). With a few exceptions, the moment arms calculated using the optimized muscle–tendon paths were generally smaller in magnitude than the moment arms reported in the literature. In four instances, optimized moment arms were opposite in function from those reported in the literature. This includes the ab/adduction moment arms of FPB at the CMC joint (reported to be an abductor but the optimized muscle path yields an adductor) in both lateral and opposition pinch, the ab/adduction moment arm of OPP at the CMC joint (reported to be an abductor, estimated to be an adductor) in lateral pinch only, and the flexion moment arm of ADPt (reported to be a flexor at the MCP joint but estimated to be an extensor) in lateral pinch. Importantly, while the moment arms estimated for the intrinsic muscles differed from the one experimental study characterizing these data in cadaveric specimens, the optimized muscle–tendon paths of the intrinsic muscles effectively replicated the force produced at the thumb-tip by each of the five intrinsic muscles, measured in a separate cadaveric study. Specifically, the endpoint forces produced individually by ADPo, ADPt, and APB matched the mean of the experimental data. Similarly, the optimized endpoint forces for FPB and OPP fell within 1 standard deviation of the experimental data, except for OPP in opposition pinch, which fell outside of 1 standard deviation by 6 degrees (Fig. 5).

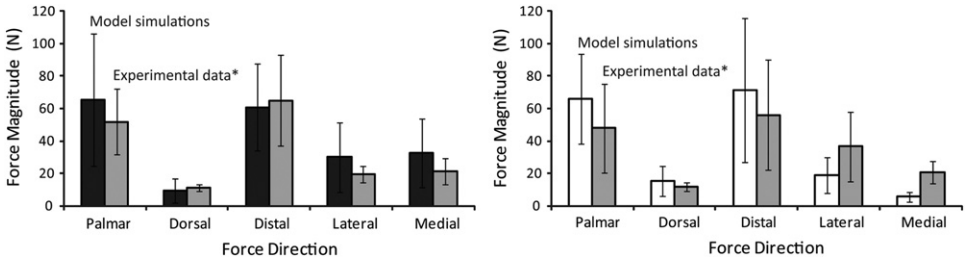

Fig. 3. Force magnitudes produced in each of five force directions, when the thumb was positioned in the lateral (left) and opposition (right) pinch posture, during coordinated muscle action. Simulation results are indicated in black (lateral pinch, left) and white (opposition pinch, right). Experimental human subject data as reported in Valero-Cuevas et al. (2003) are shown in gray. Error bars indicate ± 1 standard deviation from the mean.

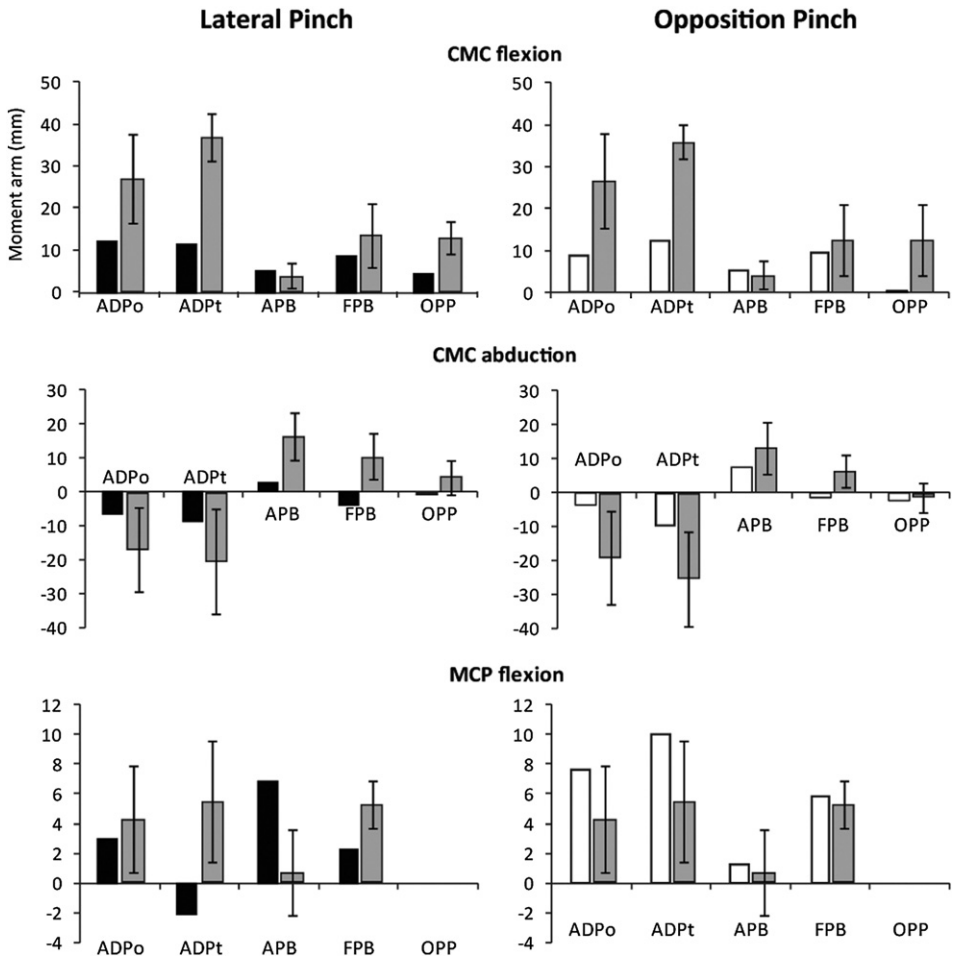

Fig. 4. Moment arms generated from the muscle path optimization versus literature moment arm values (Smutz et al., 1998) in lateral (left) and opposition pinch posture (right) for the three degrees of freedom the intrinsic muscles cross, CMC flexion/extension (top, flexion positive), CMC abduction/adduction (middle, abduction positive) and MCP flexion/extension (bottom, flexion positive). Optimization moment arms are indicated in black (lateral pinch, left) and white (opposition pinch, right). Experimental moment arm data (Smutz et al., 1998) are shown in gray. Error bars indicate ± 1 standard deviation from the mean. OPP does not cross the MCP joint and therefore has no moment arm across MCP flexion.

Our Monte Carlo simulations suggest that the kinematic representation of the thumb implemented in the model described by Holzbaur et al. best explains the increased thumb-tip endpoint forces generated by the combined action of all thumb muscles observed in our study relative to previous work (Table 3). The model developed in this study produced thumb-tip endpoint forces that were 1.2 times stronger than human subjects data in the lateral pinch posture (see Table 3, simulation 1). In contrast, the results of the Monte Carlo simulations in which the same isometric muscle forces and moment arms were combined with the simplified kinematic representation were 44% of the strength of the human subject data (see Table 3, simulation 3). In all cases where the only factor that varied between two sets of Monte Carlo simulations was the description of the joints' axes of rotation, the simulations with the simplified axes of rotation estimated maximum forces that were on average 3.2 times less than the forces estimated with the experimental axes of rotation implemented by Holzbaur et al. (2005). The difference between any two simulations where only the parameter sub-space for maximal muscle forces varied, simulations with maximal muscle forces estimated from PCSAs measured in cadaveric specimens were 1.8 times less than simulations with maximal muscle forces estimated from imaging muscle volumes in human subjects. The difference between any two simulations where only moment arms varied were equivalent on average.

4. Discussion

In this study, we describe simulations performed using a biomechanical model of the thumb that successfully reproduce the magnitude of forces produced at the thumb-tip by human subjects. Our sensitivity study confirms the hypothesis that simplifying the axes of rotation in a biomechanical model of the thumb places substantial limitations on the magnitude of the simulated force at the thumb-tip during coordinated muscle action. Therefore, the choice of representation of the joint axes of rotation is of critical importance for replicating coordinated force production by the muscles of the thumb. Here, we broadly demonstrate that our biomechanical simulations more closely replicate forces produced by human subjects when the axes of rotation better reflected experimental data (Hollister et al., 1992, 1995).

Notably, our simulation study also revealed that the moment arms of the intrinsic muscles necessary to accurately replicate the endpoint forces produced when individual cadaveric muscles were loaded with a known force did not fall within the range of moment arms reported by Smutz et al. (Fig. 5). Instead, our optimized muscle–tendon paths are associated with moment arms that are smaller across all degrees of freedom and, in some cases, are the opposite of the mechanical actions reported in the experimental moment arm study. Furthermore, the simulated endpoint forces for the individual intrinsic muscles were nearly 4 times greater than the

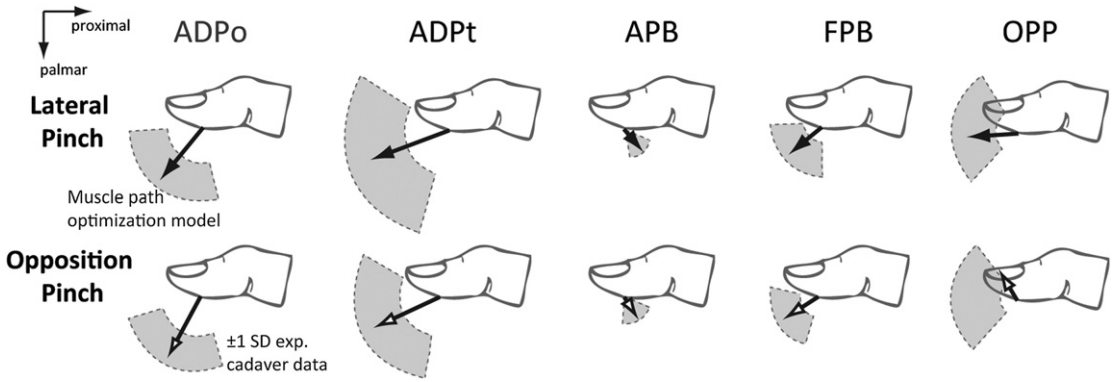

Fig. 5. Thumb-tip endpoint forces in the proximal-palmar plane in lateral (top) and opposition pinch posture (bottom) for all intrinsic muscles. The gray region represents one standard deviation of both magnitude and direction of the experimental cadaver endpoint force data (Pearlman et al., 2004). The black arrows (lateral pinch, top) and open arrows (opposition pinch, bottom) represent the endpoint force generated using the muscle path optimization method.

Table 3
Sensitivity of force magnitudes to different parameter sub-spaces in lateral pinch.

Simulation number	Joint kinematics	Moment arms	Maximal muscle forces	Times stronger than human subject data	
				Mean	SD
1	Experimentally based[a]	Model	Imaging[b]	1.22	0.32
2	Experimentally based[a]	Model	Cadaveric[c]	0.61	0.20
3	Orthogonal and intersecting	Model	Imaging[b]	0.44	0.40
4	Orthogonal and intersecting	Model	Cadaveric[c]	0.28	0.26
5	Experimentally based[a]	Literature[d]	Imaging[b]	1.47	0.51
6	Experimentally based[a]	Literature[d]	Cadaveric[c]	0.73	0.18
7	Orthogonal and intersecting	Literature[d]	Imaging[b]	0.34	0.20
8	Orthogonal and intersecting	Literature[d]	Cadaveric[c]	0.21	0.11

[a] Hollister et al. (1992, 1995).
[b] Holzbaur et al. (2007a, 2007b).
[c] Jacobson et al. (1992).
[d] Smutz et al. (1998).

experimental data from cadaver muscles loaded with a known force (Pearlman et al., 2004) when the simulations were repeated and experimental moment arms (Smutz et al., 1998) were used in the transformation between muscle and endpoint forces (see Eq. (3)) instead of the moment arms that resulted from our optimized muscle paths. The overestimation of endpoint forces produced by individual muscles when muscle paths were modeled to replicate experimental moment arm data is consistent with previous studies (Towles et al., 2008 and Goehler and Murray, 2010). Our simulations of the endpoint forces produced by individual intrinsic muscles highlight discrepancies in the existing experimental data describing the mechanical actions of the thumb muscles collected using different cadaveric experimental methods (i.e. measurement of thumb-tip endpoint forces vs. measurement of muscle moment arms).

The muscle–tendon paths of the extrinsic muscles were unaltered from their original descriptions (Goehler and Murray, 2010; Holzbaur et al., 2005). Therefore, the current biomechanical model overestimates the endpoint forces produced by 2 of the 4 extrinsic muscles (Goehler and Murray, 2010). A similar optimization algorithm for the muscle–tendon paths of the extrinsic muscles could be implemented to gain further insight into this discrepancy. Regardless, our simulation study highlights that detailed biomechanical investigations of the thumb muscles remain few in number, the available experimental data is not mechanically consistent across different studies, and further study is needed.

The augmented model presented in this study is the first biomechanical model of the thumb that has been shown to replicate experimental measurements of endpoint forces produced by both individual muscles and force production by coordination of all the muscles of the thumb. Our results emphasize that an accurate description of the thumb joints' axes of rotation is required to simulate the endpoint forces produced when muscle actions are coordinated. In addition, we demonstrate that the endpoint forces produced by individual muscles cannot be replicated with existing experimental data describing muscle moment arms. Although we did not evaluate them in this study, we expect that the activation patterns that result from the linear programming methodology implemented here will best replicate those used by human subjects when calculated using a biomechanical model that transforms muscle force to endpoint force accurately for both individual muscles and coordinated muscle actions. The simulation results described here are a critical step toward more fully understanding how thumb muscles combine to produce coordinated thumb-tip endpoint forces. Given the complexity of the thumb, we believe that the development of an accurate biomechanical model is a necessary tool to more fully understand thumb mechanics.

Conflict of interest statement

The authors of this manuscript have no conflicts of interest to disclose.

Acknowledgments

We thank Joe Towles for helpful discussions regarding implementation of the extensor hood. We would like to acknowledge funding from the National Institute of Health (NIH R01 HD046774 and NIH R01 EB011615). Sarah Wohlman was supported, in part, by the National Science Foundation under Grant No. DGE-0903637.

References

Brand, P.W., Beach, R.B., Thompson, D.E., 1981. Relative tension and potential excursion of muscles in the forearm and hand. Journal of Hand Surgery 6, 209–219.

Delp, S.L., Loan, J.P., 1995. A graphics-based software system to develop and analyze models of musculoskeletal structures. Computers in Biology and Medicine 25, 21–34.

Goehler, C.M., Murray, W.M., 2010. The sensitivity of endpoint forces produced by the extrinsic muscles of the thumb to posture. Journal of Biomechanics 43, 1553–1559.

Hollister, A., Buford, W.L., Myers, L.M., Giurintano, D.J., Novick, A., 1992. The axes of rotation of the thumb carpometacarpal joint. Journal of Orthopaedic Research 10, 454–460.

Hollister, A., Giurintano, D.J., Buford, W.L., Myers, L.M., Novick, A., 1995. The axes of rotation of the thumb interphalangeal and metacarpophalangeal joints. Clinical Orthopaedics and Related Research 320, 188–193.

Holzbaur, K.R., Murray, W.M., Delp, S.L., 2005. A model of the upper extremity for simulating musculoskeletal surgery and analyzing neuromuscular control. Annals of Biomedical Engineering 33, 829–840.

Holzbaur, K.R., Murray, W.M., Gold, G.E., Delp, S.L., 2007a. Upper limb muscle volumes in adult subjects. Journal of Biomechanics 40, 742–749.

Holzbaur, K.R.S., Delp, S.L., Gold, G.E., Murray, W.M., 2007b. Moment-generating capacity of upper limb muscles in healthy adults. Journal of Biomechanics 40, 2442–2449.

Jacobson, M.D., Raab, R., Fazeli, B.M., Abrams, R.A., Botte, M.J., Lieber, R.L., 1992. Architectural design of the human intrinsic hand muscles. Journal of Hand Surgery 17, 804–809.

Mogk, J.P., Johanson, M.E., Hentz, V.R., Saul, K.R., Murray, W.M., 2011. A simulation analysis of the combined effects of muscle strength and surgical tensioning on lateral pinch force following brachioradialis to flexor pollicis longus transfer. Journal of Biomechanics 44, 669–675.

Pearlman, J.L., Roach, S.S., Valero-Cuevas, F.J., 2004. The fundamental thumb-tip force vectors produced by the muscles of the thumb. Journal of Orthopaedic Research 22, 306–312.

Smutz, W.P., Kongsayreepong, A., Hughes, R.E., Niebur, G., Cooney, W.P., An, K.N., 1998. Mechanical advantage of the thumb muscles. Journal of Biomechanics 31, 565–570.

Swanson, A.B., 1964. Evaluation of impairment of function in the hand. Surgical Clinics of North America 44, 925–940.

Towles, J.D., Hentz, V.R., Murray, W.M., 2008. Use of intrinsic thumb muscles may help to improve lateral pinch function restored by tendon transfer. Clinical Biomechanics 23, 387–394.

Valero-Cuevas, F.J., Johanson, M.E., Towles, J.D., 2003. Towards a realistic biomechanical model of the thumb: the choice of kinematic description may be more critical than the solution method or the variability/uncertainty of musculoskeletal parameters. Journal of Biomechanics 36, 1019–1030.

Yeo, S.H., Mullens, C.H., Sandercock, T.G., Pai, D.K., Tresch, M.C., 2011. Estimation of musculoskeletal models from in situ measurements of muscle action in the rat hindlimb. Journal of Experimental Biology 214, 735–746.